Numerical investigation of the effect of tamper weight and drop height on dynamic compaction of landfills

Ali Asghar Naemi[1], Mohammad Reza Atrechian[2*], Mohammad Hossein Taghizadeh Valdi[3]

1 Department of Civil Engineering, Central Tehran Branch, Islamic Azad University, Tehran, Iran.
2 Department of Civil Engineering, North Tehran Branch, Islamic Azad University, Tehran, Iran.
3 Department of Civil Engineering, Mehr-Aeen Higher Education Institute, Bandar Anzali, Iran.

* dr.atre@yahoo.com

Abstract

The dynamic compaction method for soil improvement was introduced by Louis Menard in 1970. Numerical studies on dynamic compaction have predominantly been conducted on dry granular soils, with less consideration given to its application in municipal solid waste compaction. The present study aims to numerically investigate the effect of tamper weight and drop height on the dynamic compaction of landfills. This was done using the finite element software Abaqus 6.14-2 in two time steps, geostatic and explicit dynamic, using the coupled Eulerian–Lagrangian approach. The study results demonstrate that increasing the drop height of a tamper with a weight of 5 t from 5 m to 30 m increases the depth of the cavity created in the soil from 12.6 cm to 50 cm, increases the stress developed in the soil from 747 kg/m² to 4111 kg/m², and increases the plastic strain from 0.16 to 1.3. Moreover, increasing the drop height for a tamper weight of 30 t from 5 m to 30 m increases the crater depth in the soil from 50 cm to 2.73 m, increases the soil stress from 4111 kg/m² to 27176.5 kg/m², and increases the plastic strain in the soil from 1.3 to 12.27. It can thus be summarized that although both the weight and the drop height of the tamper are effective in the momentum, the applied stresses, the crater depth, and the plastic strain of the landfill, the use of heavy tampers, which require high-capacity cranes, is not recommended for dynamic compaction in landfill improvement due to limitations in their use and increased project implementation costs.

Keywords:
Dynamic compaction, landfills, tamper weight, drop height, crater depth.

1. Introduction

Urbanization, industrialization, and population densities in large cities have been primarily responsible for accelerated adverse environmental impacts in the cities and their vicinity during the last few decades. A prime example of an adverse environmental impact has been the management of huge amounts of municipal solid waste brought about via the above-mentioned processes. The current scene shows that the landfills that were once utilized in and for the cities are themselves filled to overflowing. It is difficult to find alternative new waste dumping sites next to existing cities, while all landfills located far away from cities tend to increase waste

transportation costs. Another alternative is to further extend the design life of existing landfills by increasing storage capacity. Lateral extension of landfill capacity is often not feasible due to space unavailability, while vertical extension is difficult because of sustainability issues and respective legislation. Compaction of existing waste by dynamic compaction would, therefore, be a suitable option for increasing landfill capacity. Dynamic compaction is a field method whereby a large mass (6 to 36 t) is lifted by a crane to a certain height (2 to 30 m) before being released to fall under gravity. The impact of this drop compresses any loosely bedded material underneath [1]. Normally, dynamic compaction is used for compacting dry unsaturated materials, such as loose soils, municipal solid waste, gravel, and mine spoils. The compaction of loose municipal solid waste systematically reduces the volume of existing waste and creates more space for fresh waste. Gu and Lee [2] conducted numerical modeling and successfully simulated the experimental results of Oshima and Takada [3]. They suggested two methods for optimizing the depth of soil improvement. First, they suggested dropping a heavier weight from a lower height to increase the tamper's momentum. Second, they proposed optimizing the tamper contact area to increase the compaction area, K_0. Rouaiguia and Al-Zahrani [4] carried out an investigation applying Lukas dislocation theory [5] in numerical modeling toward developing an elastoplastic finite element method for fully symmetric soil responses. Thevanayagam et al. [6] formulated an analytical model for simulating behavior during soil compaction induced by land improvement methods, using energy principles governing soil liquefaction, dynamic compaction stabilization, and rock columns. Hoosmandan et al. [7] analyzed the dynamic compaction of granular soils, using the ANSYS finite element program for both linear and nonlinear elasticity models. Pak and Jahangiri [8] performed a finite-element analysis series with PISA finite-element software to evaluate the effect of effective parameters on the design of dynamic compaction operations, such as the radius, mass, height of the tamper fall, number of impacts, depth of improvement, and soil type and initial relative density. Eftekhari and Yasrobi [9] used numerical modeling of dynamic compaction operations in granular soils with FLAC software and the finite difference method to clarify ambiguities in the dynamic compaction process. Pourjanabi and Hamidi [10] numerically modeled the impact of dynamic compaction on dry sandy soils using Abaqus software and compared results with site measurements, particularly changes in maximum particle velocity with distance from the tamper center. Ghanbari and Hamidi [11] subjected dynamic compression loads affecting slopes to numerical modeling of two-dimensional slopes with various angles (45, 60, 75, and 90 degrees) using the Abaqus finite element code.

The three-dimensional finite element model developed by Mehdipour and Hamidi [12], using Abaqus software, aimed to analyze such dynamic compaction operations through a Mohr–Coulomb model. Flat and conical rammers at different angles were modeled to determine their effects on the efficiency of dynamic compaction in distinct soils in terms of initial relative densities. According to Wang et al. [13], a two-dimensional axial model developed numerically in LS-DYNA software aims to study how landfill material properties and dynamic compaction affect deformation at the landfill surface. Kundu and Viswanadham [14] evaluated the efficacy of dynamic compaction in landfill sites through FE analysis, using the Drucker–Prager method and the Arbitrary Lagrangian–Eulerian (ALE) model. The results demonstrate waste compaction and volumetric consolidation due to dynamic compaction over various energy ranges, with corresponding ram radii and waste compactibility. Rathnayaka and Kulathilaka [15] carried out

dynamic compaction on waste materials to enhance their compaction properties. Their studies examined laboratory dynamic compactions on municipal solid waste, followed by tests on compaction properties. The results highlighted that dynamic compaction considerably enhances the compaction properties of MSW. Woods et al. [16] consider dynamic compaction an acceptable method for landfill improvement. In their findings, dynamic compaction features as a land improvement technique, especially aimed at landfill in-place material, to a level that allows vertical construction to proceed without unreasonable long-term settlements. Successful methods used to measure the effectiveness of dynamic compaction include embankment loading tests, plate loading tests, and, where necessary, post-remediation excavations. Kim [17] sought to improve the soil in a dredged landfill on the west coast of South Korea using the dynamic compaction method.
The dimensions of the tested soil box were 1 × 2.4 × 3 m, and the number of dynamic compaction stages was set to six, with five blows delivered in each stage. The study results found that excess pore water pressure began to converge in stage three (Nd = 15) after ramming. Vertical changes in pore water pressure were up to 4 m and horizontal changes up to 3 m. The resistance to cone penetration in each ramming stage increased by factors of 1.3, 1.7, and 1.1 in the second (Nd = 10), third (Nd = 15), and sixth (Nd = 30) stages, respectively. The improvement depth coefficient (α) ranged between 0.26 and 0.52, with an average of 0.39. Du et al. [18] investigated experimental and analytical modeling of ground displacement induced by dynamic compaction in granular soils. Their results showed that the shape of the crater is related to the energy level and the tamping number, and the slope and depth of the crater could directly reflect changes in tamping parameters; when the crater depth was large, the corresponding internal displacement was also large. Therefore, the geometric parameter of the crater can be seen as the link between tamping parameters and internal displacement. Bayat et al. [19] investigated the optimization of the dynamic compaction procedure for sandy soils. Their results indicated that the maximum allowed values of tamper mass and the number of tamper drops were required to minimize compaction energy. The ratio of compaction energy in a diamond pattern to that in a square pattern was also found to be about 0.75 to 0.90 under the same compaction conditions. Debeleac et al. [20] conducted an experimental and numerical study on dynamic compaction of weakly cohesive soils. Their study described the behavior of soil-drum interaction through lumped parameter modeling. The amplitude of the vertical motion was evaluated for dynamic conditions using rheological models (generalized and advanced Kelvin–Voigt-based models) and compared with experimental results from weakly cohesive soil compaction. Different modeling approaches were considered, and the results revealed that soil input properties play a vital role in modeling accuracy. Zhang et al. [21] investigated the effect of soil parameters (angle of internal friction, cohesion, modulus of elasticity, Poisson's ratio, density) on the amount of ramming settlement of rammed reinforced foundations and proposed a prediction model for the depth of ramming reinforcement based on a GA-BP neural network. Their results showed that the compaction rate is most sensitive to the internal friction angle and cohesive force. Compared with the traditional BP model, the GA-BP model has better prediction accuracy and generalization ability, with a fitting accuracy reaching 0.974. Chao et al. [22] investigated loess foundation behaviour under high-energy dynamic compaction based on experimental data. Their results demonstrated that theoretical calculations and numerical models are applicable to loess foundation tamping. At the same energy level, the horizontal reinforcement distance of the loess foundation exhibits a semi-elliptical pattern along

the depth, and the growth rate of foundation settlement initially increases and then decreases as the tamper energy level rises. When only the tamper energy level changes while other parameters remain unchanged, soil settlement is positively correlated with the energy level. However, as the energy level increases, the rate of increase in settlement and reinforcement distance gradually diminishes. Based on simulations and a comparative analysis of single- and seven-strike scenarios, the horizontal displacement of the soil surrounding the tamper is positively correlated with the number of strikes. Moreover, as the contact time between the tamper and the foundation increases, both vertical and horizontal displacements also increase.

In the dynamic compaction process, the energy imparted to the soil is a function of two primary parameters: tamper weight (W) and drop height (H), derived from the fundamental impact energy relation $E = W \times H$. Although this relation is linear, the effect of these two parameters on the final compaction of the landfill (evaluated by criteria such as permeability, bearing capacity, or settlement potential) is often nonlinear and interdependent. Conventional studies typically investigate effects by holding one variable constant (e.g., weight) while varying the other (height). This approach overlooks the complex interaction between weight and height. For instance, increasing the drop height for a given weight may improve compaction up to a specific threshold, beyond which efficiency diminishes due to localized over-compaction or shear failure. This threshold itself is a function of the tamper weight. Therefore, optimizing the process design requires a simultaneous understanding of the effects of both parameters and their interaction. A review of prior studies indicates that while the separate influence of tamper weight and drop height on compactibility has been investigated, a systematic examination of their combined and interactive effects has received less attention. Conclusions drawn from these single-variable studies may lack generalizability and accurate predictive power under practical conditions where both parameters are variable. Thus, the innovation of the present study is the investigation of the simultaneous and combined effect of tamper weight and drop height on effective parameters of dynamic compaction of landfills, such as applied stress, crater depth, plastic strain, and deformation.

2- Material and method

The numerical modeling of dynamic compaction is primarily restricted to dry, unsaturated, and thoroughly drained granular soils. Machado et al. [23] and Reddy et al. [24] studied the particle size distribution of municipal solid waste. They revealed that over 90% of the particles found in municipal solid waste are larger than 0.075 mm. In addition, the hydraulic conductivity studied by Powrie and Beaven [25] revealed values for fresh municipal solid waste ranging from 4×10^{-8} m/s to 6×10^{-8} m/s; generally, this type of material is considered to have low potential for generating unsaturated pore water pressure. This indicates that fresh municipal solid waste behaves like granular soils. Hence, due to their close resemblance, dynamic compaction modeling of municipal solid waste can successfully use the relationships established and developed for granular soils. In this research, MSW is consequently treated as an elastoplastic material and modeled using the cap plasticity model to simulate dynamic compaction behavior in soils. This model predicts the hardening behavior of soil and is applicable for dynamic problem prediction. Thus, the cap plasticity model is especially used for predicting soil behavior due to impact loading [24, 2]. The dynamic compaction process in granular soils is also modeled using the cap plasticity model with

a linear shear surface [2, 26, 27]. Cap plasticity was first conceptualized and defined by Dimaggio and Sandler [28]. Their yield surface consists of a failure cap, a moving cap, and a tension cutoff. The shear failure cap consists of two shear yield surfaces, initially a Drucker–Prager cap uniformly connected to a von Mises cap. Poran and Rodriguez [29] proposed the concept of a discrete shear yield surface to predict soil performance in dynamic compaction analysis. For a dynamic modeling approach to tamper mass impact on municipal solid waste, three kinds of numerical techniques can be applied: 1) free fall of the tamper mass from a suitable height (h) under gravity; 2) simulation of impact velocity on the tamper mass with respect to the initial velocity, V_0 ($V_0=\sqrt{(2gh)}$); 3) application of half-sine stress under the tamper, as documented by Pan and Selby [26]. In the present study, the second method was adopted, where multiple impact blows were simulated by repeatedly applying the impact velocity to the tamper mass. In the Abaqus model, cap plasticity offers a dual criterion for defining the yield surface. The first criterion is a linear shear yield surface developed according to the Drucker–Prager failure criterion of equation (1), which is defined in the context of the first and second invariants of the stress tensor (J_1 and $\sqrt{(J_2D)}$). The second yield criterion (f_2) is a movable cap defined by equation (2) to express yield and plastic volumetric strains under isotropic effective stress [8]. The cap plasticity yield surfaces are shown in Figure 1 in the J_1–$\sqrt{(J_2D)}$ plane.

$$f_1 = \sqrt{j_{2D}} - \alpha J_1 - \kappa = 0 \tag{1}$$

$$f_2 = (J_1 - l)^2 + R^2 J_{2D} - (X - l)^2 = 0 \tag{2}$$

where α and κ are the material parameters or constants of the Drucker–Prager failure criterion constituted by the internal friction angle (φ) and cohesion (c). Equations (3) and (4) are used for their formulation. The hardening parameter X, which is a material constant, and R, which is the ratio of the major axis to the minor axis of the cap curve, determine the cap's shape. The value of R depends on the shape and size of the yield cap. l is the first invariant of the stress tensor (J_1) at the intersection point of the shear failure envelope and the cap; this value is obtained at each step in terms of the hardening parameter X from equation (5). J_2D is the second invariant of the deviatoric stress tensor [30].

$$\alpha = \frac{2\sin\varphi}{\sqrt{3}\,(3-\sin\varphi)} \tag{3}$$

$$\kappa = \frac{6\,c\cos\varphi}{\sqrt{3}\,(3-\sin\varphi)} \tag{4}$$

$$l = \frac{X-\kappa.R}{1+\alpha.R} \tag{5}$$

The cap expands at each step due to the hardening law for plastic volumetric strain (ε_v^p) and is determined by equation (6).

$$X = -\frac{1}{D} Ln\left(1 - \frac{\varepsilon_v^p}{w}\right) + X_0 \tag{6}$$

where D and W are material parameters that can be determined from hydrostatic pressure tests. Low values of D and W indicate that the soil has high compressibility. ε_v^p is the plastic volumetric strain, and X_0 is the initial cap pressure from gravitational analysis. These different values are

calculated at different soil depths (h) based on the soil unit weight (γ) and the at-rest earth pressure coefficient (K_0) according to equation (7) [31].

$$X_0 = \frac{\gamma h(1+2K_0)}{3} \quad (7)$$

The initial cap parameter (X_0) was selected based on gravity analysis. Thus, X_0 varies for every line of elements in the grid due to the variation of in-situ stresses with depth. Besides, the soil elasticity parameters such as β and γ are based on values proposed by Pouran and Rodriguez [17], while parameters regarding the cap plasticity model of the soil, such as W, R, and D, are based on values proposed by Li and Guo [2], Oshima and Takada [3], and Ghasemi et al. [32] and are shown in Table 1.

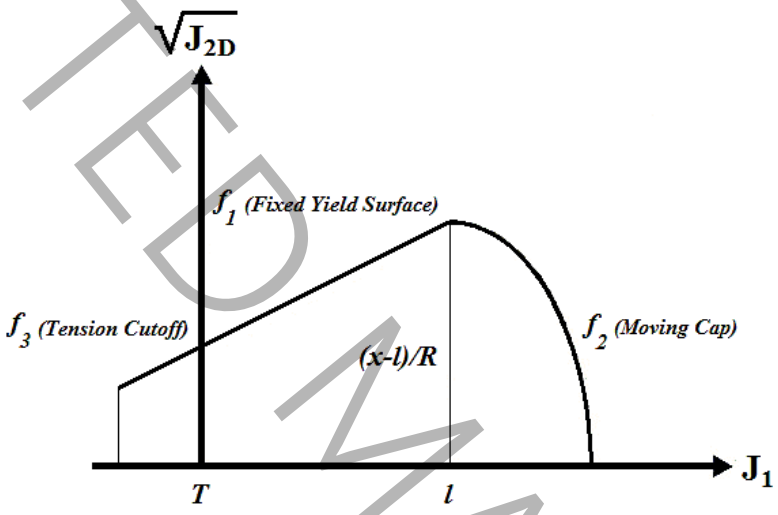

Figure 1: Yield surface of the cap plasticity model

Table 1: Cap elasticity and plasticity model parameters and Drucker-Prager constants

Elasticity model parameters			Drucker-Prager constants		Cap plasticity model parameters		
ν	β	δ	κ	α	R	W	D (m^2/kg)
0.35	6	0.025	0	0.273	3.65	0.7	0.0025

A hardening cap must be defined for the cap plasticity model to address the soil's nonlinear behavior. A model of this nature is based on limit state theory and the basic premise of a logarithmic relationship between the mean effective stress and the porosity ratio. The stress–strain diagram of the soil hardening cap model is shown in Figure 2.

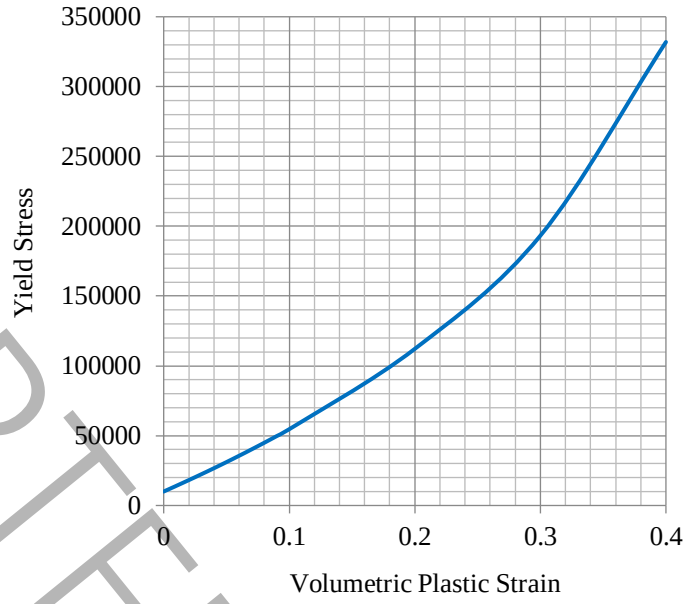

Figure 2: Stress-strain diagram of the soil hardening cap model

Initially, a dynamic analysis with an explicit time definition is set up. The numerical analysis carefully selects its sub-time step to achieve the desired numerical stability. A very large time step can cause numerical divergence, whereas a very small time step increases computational overhead [8]. Due to the large deformations, the nonlinear geometric option is activated to update the element stiffness matrix at each solution time step. Outputs were selected for the whole model domain. In the next step, the soil–tamper interaction is defined as a contact type. In the initial step, a surface-to-surface contact with the mechanical constraint formulation of the penalty contact method is chosen. The most accurate method for numerically modeling tamper–soil contact is using a contact formulation between two or more moving bodies. For simplicity, the current numerical model adopts a rigid body method to model the impact. This means that for the present application, the input to the program is the initial velocity of the tamper nodes, determined at the moment of impact with the model bed. The Young's modulus and Poisson's ratio of the ram are such that its rigidity relative to the soil mass is guaranteed at the time of impact [9]. Hence, the definition of the soil–ram interaction elements is vital for accurate modeling and energy transfer from the ram to the soil. The penalty approach in Abaqus can define those elements with a friction coefficient. The friction coefficient is tan δ, with the friction angle (δ) between the soil and the ram ranging from 1/2 φ to 2/3 φ. The value of this friction coefficient within the specified range has little effect on the results [32]. Therefore, the soil–ram interaction is a contact type, its tangential behavior defined by the penalty treatment with a friction coefficient of tan (2/3 φ), while its vertical behavior is defined by a pressure condition set as "hard contact." The next step defines the projectile mass and its rotational moment of inertia in all three X, Y, and Z directions. A non-reflective Eulerian boundary is assigned to the sides of the computational domain. These boundary conditions are specific to the Eulerian method and cause waves propagated due to the projectile's impact with the soil surface to be absorbed by the boundaries before returning to the computational domain, effectively simulating an infinite domain.

In a subsequent step, the imparted velocity upon the soil surface at the moment of contact from the numerical simulation of the tamper impact is assigned to the tamper via an explicit dynamic step with velocity/angular velocity boundary conditions. The saturated and porosity ratios of the soil are then defined. The geostatic state of the soil, previously analyzed and stored, is simulated in the first time step under the mechanical category and stress type using the specifications of the output database file and by selecting the geostatic soil state simulation file. In this step, one also defines the time step number of the geostatic state simulation of the soil and its increment. Finally, the dimensions and type of meshing for the computational domain of the soil are defined. The mesh grid is distributed from fine in the area of tamper impact to coarser at the side boundaries to accurately capture the extent of stresses and deformations. The accuracy of the solutions and the successful simulation of dynamic problems depend on the element size. Coarse elements are stiffer than fine ones. The shape of the element also influences the numerically calculated solution. Long and/or sharply angled elements can adversely affect accuracy. This is especially true when large deformations occur because elements can become badly stretched or angled, which compromises the simulation. The element size and time increment are strongly related parameters that must be considered together, and particular attention must be given to the selection of element size and shape. Thus, for wave propagation problems in a dynamic compaction model, grid resolution must be chosen very cautiously. Too small an element size may induce numerical instability, while large elements may not permit the transfer of smaller waves associated with higher frequencies. Moreover, the time increment must be selected such that it allows the fastest wave (the compression wave) to propagate between two immediate nodes within the time step. To overcome the limitations of one-factor-at-a-time methods, this study employs a full two-factor factorial experimental design. In this design, different levels of tamper weight (5, 10, 15, 20, 25, and 30 tonnes) and different levels of drop height (5, 10, 15, 20, 25, and 30 meters) are applied simultaneously in all possible combinations (36 combinations). This approach enables the isolation and quantification of three components:

1. Main effect of tamper weight
2. Main effect of drop height
3. Interaction effect between weight and height (W × H)

Analysis of the results will determine whether the interaction effect between these two factors is statistically significant. This would mean that the impact of changing the height depends on the selected weight level, and vice versa.

The reason for choosing this number of models is to investigate the effect of the tamper's weight and drop height on the stresses applied to the landfill, the crater depth, and the plastic strain created in it. Specifically, the study examines the effect of the tamper on these parameters under different weights and drop heights. For instance, it explores what happens if the tamper weight is low but its drop height is maximum, or if the weight is high but the drop height is minimum, in terms of the resulting stresses, crater depth, and plastic strain.

The mesh defined in Abaqus for the analysis is depicted in Figure 3. The model comprises two discrete parts: the tamper and the mass-spring-damper (MSD). The tamper is a cylindrical mass. Both the impact mass and the mass-spring-damper model have been modeled with bilinear axisymmetric isoparametric elements.

In Figure 3, two portions are represented: ABCD represents municipal solid waste placed 18 m under the landfill with a 14 m horizontal extension. The region AEFG shows the tamper with a radius varying from 0.6 m to 1.5 m. GAD is the symmetry line, so all nodes on that line are constrained in the x-direction, while nodes on lines CD and BC are constrained in the y and x directions, respectively. To characterize deformations and stresses well, a mesh size of 0.2 × 0.2 m^2 was used at the point of impact, with larger mesh sizes elsewhere. Interaction between the municipal solid waste and the tamper is modeled with an assumed coefficient of friction of 0.1.

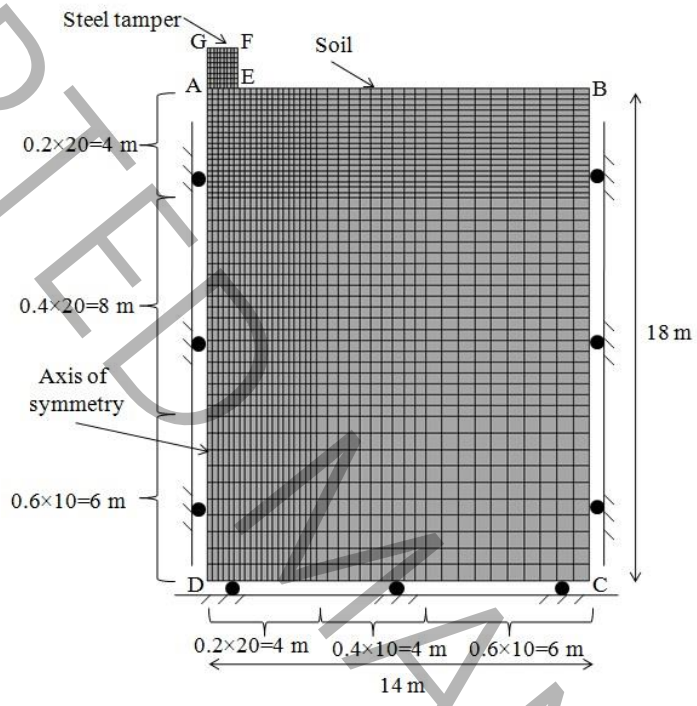

Figure 3: Meshing of the two-dimensional symmetric FE model.

Validation of the developed numerical model

The comparison between the present numerical investigation and dynamic compaction tests on municipal solid waste carried out by Reddy et al. [24] is shown in Figure 4. According to their data, the initial density, relative density, and internal friction angle for the landfill were taken as 6 kN/m^3, 35%, and 35°, respectively, and the lateral earth pressure coefficient was 0.8. As shown, the curves in the vertical stress–axial strain graphs of both studies are in good agreement, with an average discrepancy of approximately 7%.

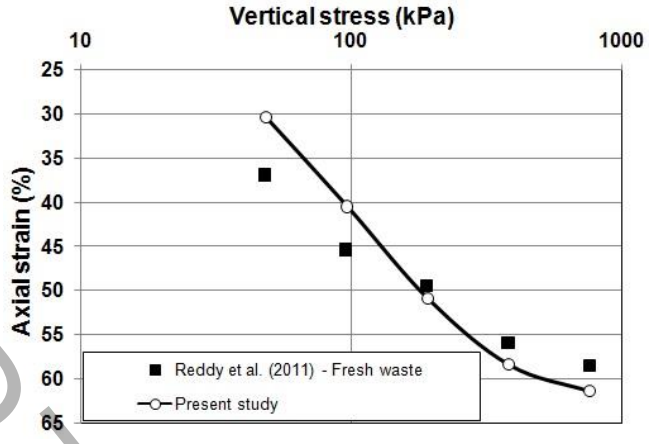

Figure 4: Comparison of the results of the present study with the laboratory results of Reddy et al. [24].

3- Results and discussion

Figure 5 shows the variation of stress with the tamper's drop height from the landfill surface. As shown, increasing the drop height of the 5-t tamper from 5 m to 30 m increased the stress induced in the landfill from 747 kg/m² to 4111 kg/m², an increase of 550%. Increasing the drop height of the 10-t tamper from 5 m to 30 m increased the stress from 1468.83 kg/m² to 7947.33 kg/m², a 541% increase. Similarly, for the 15-t tamper, the stress increased from 2172.99 kg/m² to 11532.2 kg/m², a 530% increase. For the 20-t tamper, the stress went from 2857.12 kg/m² to 19836 kg/m², a 694% increase. For the 25-t tamper, the stress increased from 3518.62 kg/m² to 23656.3 kg/m², a 672% increase. Finally, for the 30-t tamper, the stress increased from 4111 kg/m² to 27176.5 kg/m², a 661% increase. The results show that as the drop height increases, the energy transferred from the tamper to the landfill increases due to the higher speed at the moment of impact. Thus, greater stress occurs in the landfill. Since momentum is the product of mass and velocity, it can be seen that when the 5-t tamper is released from a height of 5 meters and impacts the landfill surface, it has the lowest momentum compared to tampers with higher weights and drop heights. Consequently, the stress applied to the landfill, as well as its crater depth and deformation, are minimal. By increasing the drop height of the 5-t tamper to 30 meters, its impact speed and momentum increase, resulting in a significant increase in the applied stress, crater depth, and deformation. On the other hand, when the 30-t tamper is released from a height of 5 meters, its speed at impact is low, giving it the lowest momentum compared to tampers with higher drop heights. As a result, the crater depth and deformation of the landfill are minimal. Finally, when the 30-t tamper is released from a height of 30 meters, its high speed at impact gives it the maximum momentum compared to tampers with lower weights and drop heights, leading to the maximum crater depth and deformation.

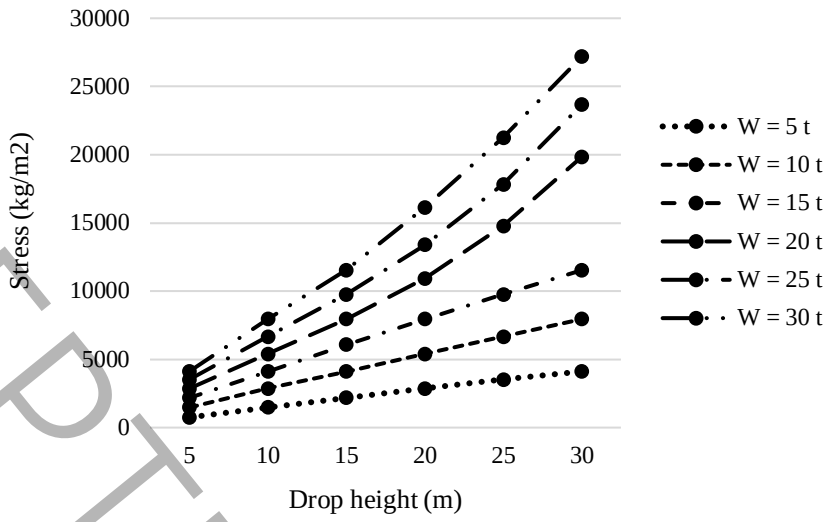

Figure 5: Diagram of the maximum stress created in the landfill due to changes in the weight and drop height of tampers.

Figure 6 shows the maximum crater depth due to changes in tamper weight and drop height. Increasing the drop height of the 5-t tamper from 5 m to 30 m increases the crater depth from 12.6 cm to 50 cm, a 296% increase. For the 10-t tamper, the depth increases from 20.3 cm to 96.5 cm (375%). For the 15-t tamper, from 28 cm to 1.41 m (403%). For the 20-t tamper, from 35.68 cm to 1.86 m (421%). For the 25-t tamper, from 43 cm to 2.30 m (434%). For the 30-t tamper, from 50 cm to 2.73 m (446%). The reason is that the tamper has a higher speed at the moment of striking the landfill surface. Based on the relationship $V=\sqrt{(2gh)}$, as the drop height (h) increases, the tamper's velocity (V) at impact increases, and consequently, its momentum increases. In addition to transferring impact energy to the lower layers of the landfill, this leads to a decrease in porosity and the space between its components, resulting in an increased crater depth. Therefore, the momentum delivered during the tamper drop plays an equally important role in governing the overall efficiency of dynamic compaction.

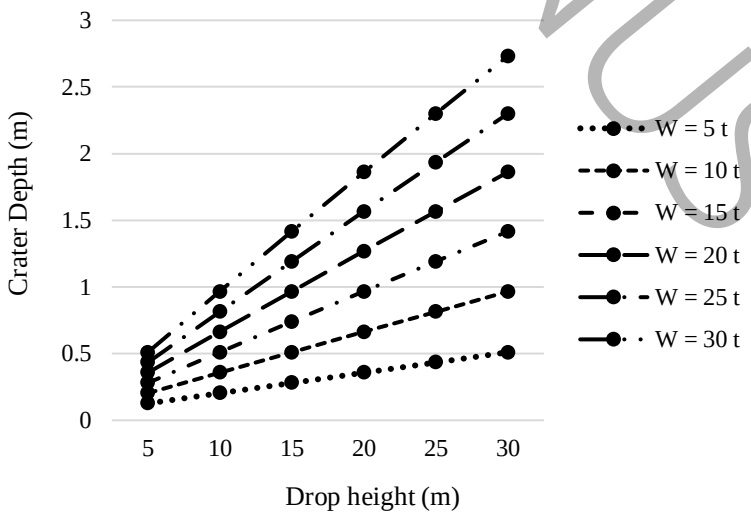

Figure 6: Diagram of the maximum crater depth due to changes in the weight and drop height of tampers.

Figures 7 and 8 show the contours of landfill deformation due to the impact of tampers with different weights and drop heights, and the variation in landfill plastic strain with increasing tamper weight and drop height, respectively. As can be inferred, increasing the drop height of the 5-t tamper from 5 m to 30 m increases the plastic strain in the landfill from 0.16 to 1.3, an 812% increase. For the 10-t tamper, plastic strain increases from 0.44 to 2.76 (627%). For the 15-t tamper, from 0.67 to 5.29 (789%). For the 20-t tamper, from 0.9 to 7.43 (825%). For the 25-t tamper, from 1.11 to 9.57 (862%). For the 30-t tamper, from 1.3 to 12.27 (943%). This shows that with increasing drop height, the tamper's velocity and momentum at impact increase, transferring more energy to the landfill. As a result, further reduction in porosity and empty spaces between its components leads to increased settlement and plastic strain. The effect of increasing the tamper's weight and drop height on the rate of landfill improvement can be explained by the fact that increasing these parameters increases the efficiency of energy transferred to the landfill. For a given energy per impact, using a lighter weight and a lower drop height decreases momentum, while using a heavier weight and a higher drop height increases momentum. Ideally, considering the landfill mass as the target, if the impact momentum is greater, more energy is transferred to the landfill. Therefore, at a given energy level per impact, increasing the weight and drop height of the tamper increases momentum and, consequently, the efficiency of the dynamic compaction operation. The results show that at high drop heights with the minimum weight, and at low drop heights with the maximum weight, the difference in impact depth is relatively small. Therefore, both the weight and the drop height of the tamper are effective in determining the applied stresses, crater depth, and plastic strain of the landfill, so a deficiency in any of these factors can lead to failure to achieve the required compaction. Thus, to apply the dynamic compaction method for landfill improvement, the use of heavy tampers, which require high-capacity cranes, is not recommended due to practical limitations and increased project implementation costs. The practical suggestion of this article is to focus on increasing the drop height of the tamper rather than its weight. By increasing the drop height, the impact speed and consequently the applied stresses increase, leading to greater crater depth and plastic strains in the landfill.

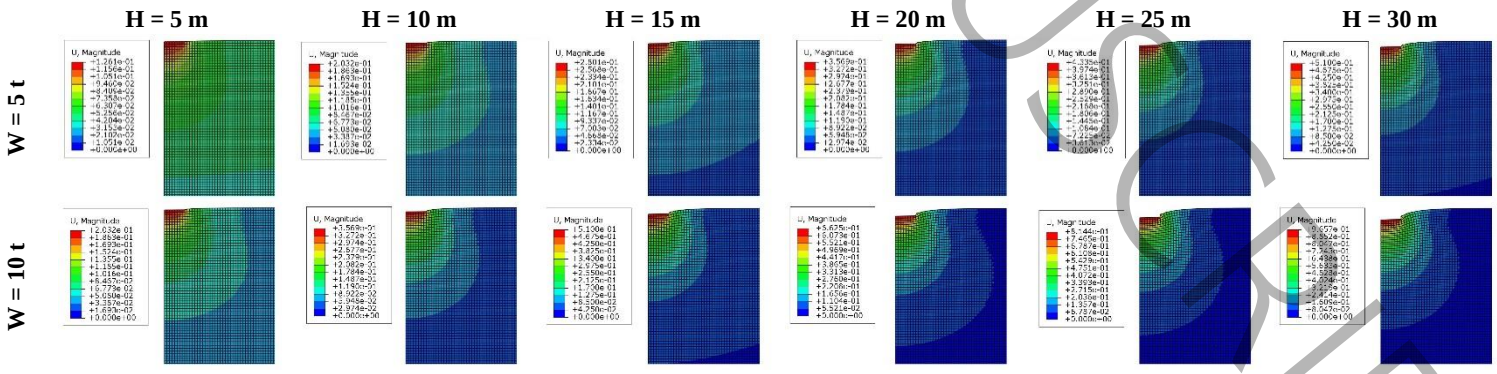

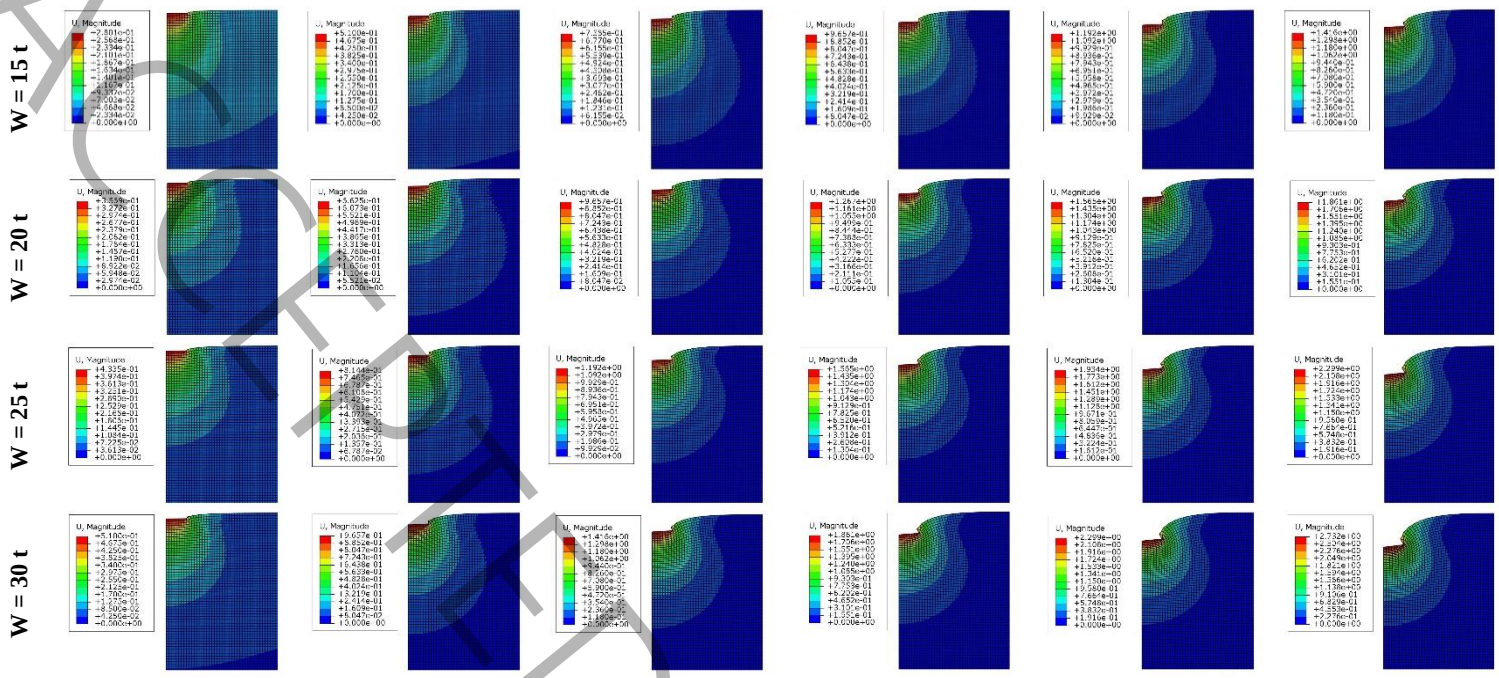

Figure 7: Contours of deformation created in the landfill with changes in weight and drop height of tampers.

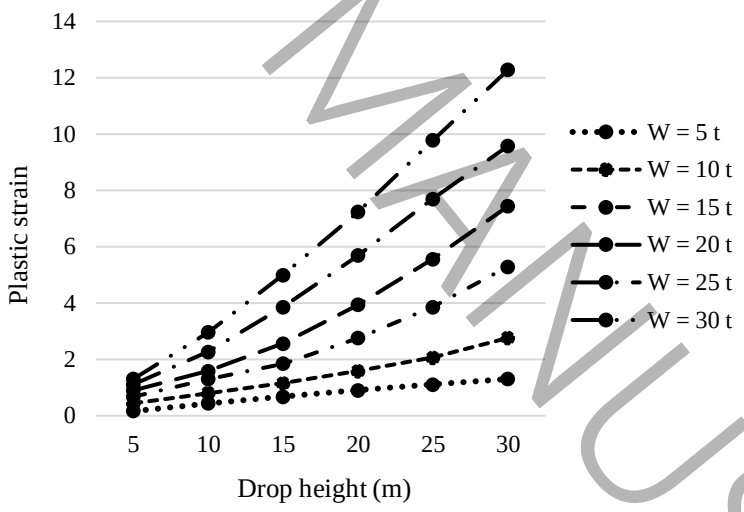

Figure 8: Diagram of the maximum plastic strain created in the landfill due to changes in the weight and drop height of tamper.

4. Conclusion

The present study aimed to investigate the efficacy of the dynamic compaction process in reducing the volume of municipal solid waste accumulated over time. The study is especially relevant due to the acute shortage of space in urban areas, which makes finding new landfill sites for waste disposal challenging. Finite element-based studies were conducted using the commercial software Abaqus (ver. 6.14-2), employing the Drucker–Prager constitutive law and a coupled Lagrangian–Eulerian remeshing approach. This study focused on the effect of tamper weight and drop height

on the dynamic compaction of landfills. For this purpose, tamper weights of 5, 10, 15, 20, 25, and 30 tonnes and drop heights of 5, 10, 15, 20, 25, and 30 meters were considered. The validity of these numerical models was confirmed through comparison with experimental results obtained by Reddy et al. [24]. The results showed that when the 5-t tamper is released from a height of 5 meters, it has the lowest momentum compared to other tampers, resulting in minimal applied stress, crater depth, and plastic strain. Increasing its drop height to 30 meters significantly increases its impact speed and momentum, leading to substantial increases in stress, crater depth, and plastic strain. Conversely, when the 30-t tamper is released from 5 meters, its low speed results in minimal momentum, crater depth, and plastic strain. Releasing it from 30 meters yields the highest speed and momentum, producing the maximum crater depth and plastic strain. Although both tamper weight and drop height are effective in determining momentum, applied stresses, crater depth, and plastic strain, the use of heavy tampers requiring high-capacity cranes is not recommended for dynamic compaction in landfill improvement due to practical limitations and increased costs. The study suggests focusing on optimizing drop height as a more practical and cost-effective parameter.

5- Appreciation

The authors sincerely thank and appreciate the cooperation and guidance of Dr. Mahmood Vafaeian in this article.

6. References

[1] M.H. Taghizadeh Valdi, M.R. Atrechian, A. Jafary Shalkoohy, S.A. Hosseini, Experimental study of the effect of holes number and arrangement of lattice pounder on offshore dynamic compaction, Amirkabir Journal of Civil Engineering, 52(8) (2020) 1923-1934.

[2] Q. Gu, F.H. Lee, Landfill response to dynamic compaction. Journal of Geotechnique, 52(7) (2002) 481- 493.

[3] A. Oshima, N. Takada, Relation between compacted area and ram momentum by heavy tamping, Proceedings of 14th ICSMFE, 1994, pp. 1641–1644.

[4] A. Rouaiguia, R. Al-Zahrani, Simulation of soil dynamic compaction. The 6th Saudi Engineering Conference, 2002, pp. 223-232.

[5] R.G. Lukas, Dynamic compaction for highway construction, Volume 1: Design and Construction Guidelines, Federal Highway Administration, FHWA Report Rd-86/133. 1986.

[6] S. Thevanayagam, G. Martin, R. Nashed, T. Shenthan, T. Kanagalingam, N. Ecemis, Liquefaction remediation in silty soils using dynamic compaction and stone columns, University of Buffalo Publishing, 2006, pp. 118.

[7] R. Hoosmandan, S.S. Yasrobi, A. Pak, Prediction of soil improvement in dynamic compaction operations by adjusting pounder penetration values, Modares Journal of Engineering, 28 (2007) 15-29.

[8] A. Pak, G. Jahangiri, Numerical Study of the effects of energy, momentum, and tamper radius and soil initial relative density on soil improvement by dynamic compaction, Proceedings of 5th National Congress on Civil Engineering, 2010, pp. 1-8.

[9] S. S. Eftekhari, S. Yasrobi, Landfill improvement by dynamic compaction using numerical modeling by finite difference method in dry sand, Modares Journal of Civil Engineering, 11(3) (2011) 55-65.

[10] M. Pourjenabi, A. Hamidi, Numerical modeling of dynamic compaction process in dry sands considering critical distance from adjacent structures, Journal of Structural Engineering and Mechanics, 56(1) (2015) 49-56.
[11] E. Ghanbari, A. Hamidi, Improvement parameters in dynamic compaction adjacent to the slopes, Journal of Rock Mechanics and Geotechnical Engineering, 7 (2015) 233-236.
[12] S. Mehdipour, A. Hamidi, Impact of tamper shape on the efficiency and vibrations induced during dynamic compaction of dry sands by 3D finite element modeling, Civil Engineering Infrastructures Journal, 50(1) (2017) 151-163.
[13] W. Wang, J.J. Chen, J.H. Wang, Estimation method for landfill deformation of granular soils caused by dynamic compaction, Journal of Soil Dynamics and Earthquake Engineering, 92 (2017) 266–278.
[14] S. Kundu, B.V.S. Viswanadham, Use of Dynamic Compaction for Densifying MSW Landfills, In Transportation, Water and Environmental Geotechnics: Proceedings of Indian Geotechnical Conference, 2020, pp. 159-169.
[15] R.I.A. Rathnayaka, S.A.S. Kulathilaka, Improvement of compressibility characteristics of waste material by dynamic compaction, 2021.
[16] C. Woods, R. Shaffer, S. Drumheller, Dynamic Compaction: A Proven Landfill Improvement Method for Landfill Sites, In Geo-Congress, 2023, pp. 311-321.
[17] M. Kim, Enhancing Landfill Improvement of Dredging Landfill in South Korea's Western Coastal Region: Insights into Dynamic Compaction Characteristics, Buildings, 13(7) (2023) 1830.
[18] J. Du, Y. Zhang, S. Wu, Y. Dong, J. Shi, Experimental and Analytical Modeling of Ground Displacement Induced by Dynamic Compaction in Granular Soils. Buildings, 13(2) (2023) 539.
[19] M. Bayat, M. Saadat, A. Hojati, Optimization of dynamic compaction procedure for sandy soils, Civil Engineering Infrastructures Journal, 57(1) (2024) 145-156.
[20] C.N. Debeleac, A. Buraga, S.M. Nastac, Experimental and Numerical Study in Dynamic Compaction of Weakly-Cohesive Soils, Applied Sciences, 14(22) (2024) 10129.
[21] Y. Zhang, X. Chen, H. Ge, Z. Guo, X. Li, Influence of soil parameters on dynamic compaction: numerical analysis and predictive modeling using GA-optimized BP neural networks, Frontiers in Materials, 12 (2025) 1631816.
[22] W. Chao, Y. Niu, S. Zhang, B. Gong, Numerical Simulation of Loess Foundation Behaviour Under High-Energy Dynamic Compaction Based on Experimental Data, Soil Mechanics and Foundation Engineering, 62(5) (2025) 515-522.
[23] S.L. Machado, M.F. Carvalho, O.M. Vilar, Constitutive model for municipal solid waste, Journal of Geotechnical and Geoenvironmental Engineering, 128(11) (2002) 940-951.
[24] K.R. Reddy, H. Hettiarachchi, J. Gangathulasi, J.E. Bogner, Geotechnical properties of municipal solid waste at different phases of biodegradation, Waste Management, 31(11) (2011) 2275-2286.
[25] W. Powrie, and R.P. Beaven, Hydraulic properties of household waste and implifications for landfills, Proceedings of the Institution of Civil Engineers Geotechnical Engineering, 137(4) (1999) 235-247.
[26] H.S. Thilakasiri, M. Gunaratne, G. Mullins, P. Stinnette, C. Kuo, Implementation aid for dynamic replacement of organic soils with sand, Journal of Geotechnical and Geoenvironmental Engineering, 127(1) (2001).
[27] A. Pak, H. Shahir, A. Ghassemi Behavior of dry and saturated soils under impact load during dynamic compaction, Proceedings of the 16th ICSMGE, 2005, pp. 1245-1248.

[28] F.L. Dimaggio, I.S. Sandler, Material model for granular soils, Journal of Engineering Mech. 97 (1971).
[29] C.J. Poran, J. Rodriguez, A finite element analysis of impact behavior of sand, Journal of Soils and Foundations, 32(4) (1992) 68-80.
[30] J.L. Pan, A.R. Selby, Simulation of dynamic compaction of loose granular soil, Journal of Advances in Engineering Software, 33 (2002) 631-640.
[31] E. Ghanbari, A. Hamidi, Numerical modeling of rapid impact compaction in loose sands, Journal of Geomechanics and Engineering, 6(5) (2014) 487-502.
[32] A. Ghassemi, A. Pak, H. Shahir, A numerical tool for design of dynamic compaction treatment in dry and moist sands, Iranian Journal of Science and Technology, Transaction B, Engineering, 33(B4) (2009) 313-326.